Sustainable Ammonia Production from Nitrate Reduction Assisted by Methanol Oxidation Using Co@CF Bifunctional Electrocatalysts

Xunniu Cheng[a+], Zixuan Xie[a+], Shilin Zha[a], Qiuhua Xu[a], Suqin Ci[c,*], Zhenhai Wen[a,b,*]

a Key Laboratory of Jiangxi Province for Persistent Pollutants Control, National-Local Joint Engineering Research Center of Heavy Metals Pollutants Control and Resource Utilization and Resources Recycle, Nanchang Hangkong University, Nanchang, 330063, Jiangxi, China

b State Key Laboratory of Structural Chemistry, and Fujian Provincial Key Laboratory of Materials and Techniques toward Hydrogen Energy, Fujian Institute of Research on the Structure of Matter, Chinese Academy of Sciences, Fuzhou, Fujian, 350002, China.

c Fujian Provincial Key Laboratory of Soil Environmental Health and Regulation, College of Resources and Environment, Fujian Agriculture and Forestry University, Fuzhou 350002, China

[+] *These authors contributed equally to this work*

** Corresponding authors*

E-mail: wen@fjirsm.ac.cn, sqci@fafu.edu.cn

Synthesis procedure

Pretreatment of copper foam involves cutting it to a size of 2x3cm^2 and then ultrasonic treatment. Then, the copper foam was immersed in dilute nitric acid (volume ratio of nitric acid to deionized water =1:5), ethanol and deionized water successively for 10 minutes each time.

According to the sequence of 0.5g Urea, 0.5g $HONH_2HCl$, 1g $(CH_3COO)_2Co\cdot4H_2O$, it was dissolved in 100mL deionized water and stirred for 10min. Then the pre-treated copper foam base was taken and electrodeposited for 20min at an applied voltage of -1.6V. After electrodeposition, vacuum drying in a vacuum drying oven at 60℃.

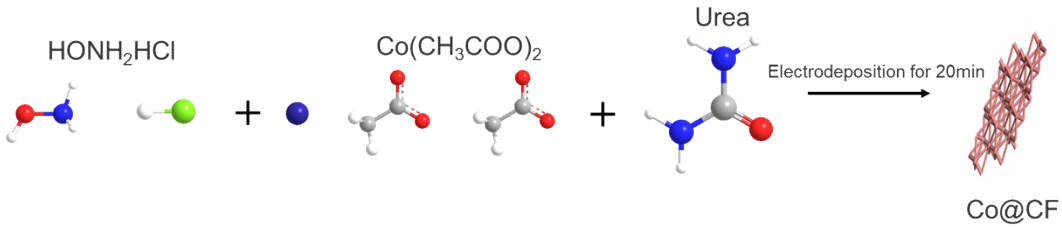

Chemicals and materials

Sodium nitrite ($NaNO_2$, 99%), Phosphoric acid (H_3PO_4, ≥85%), Sulfonamide ($C_6H_8N_2O_2S$, 99.5%), Naphthalene ethylenediamine hydrochloride ($C_{12}H_{14}N_2\cdot2H_2O$, 98%), Ammonium chloride (NH_4Cl, ≥99.5%), Sodium nitroprusside ($C_5FeN_6Na_2O\cdot2H_2O$, 99%), Salicylic acid ($C_7H_6O_3$, 99.5%), Sodium citrate dihydrate ($C_6H_5Na_3O_7\cdot2H_2O$, 99.0%), Sodium hydroxide (NaOH, 96%), Sodium Hypochlorite Pentahydrate ($NaClO\cdot5H_2O$, ≥40%) , Potassium hydroxide (KOH, ≥90%), Potassium nitrate (KNO_3, ≥99%), Ethanol (CH_3CH_2OH, 99.7%), Nitric acid (HNO_3, 65%~68%), methanol (CH_3OH, 99.5%), Dimethyl sulfoxide (C_2H_6SO, ⩾99%), Sodium formate ($CHNaO_2$, 99.5%), Cobalt(II) acetate tetrahydrate ($(CH_3COO)_2Co\cdot4H_2O$, 99%), Hydroxylamine hydrochloride ($HONH_2HCl$, 99%), Urea ($CO(NH_2)_2$, ⩾99.0%), Potassium dihydrogen phosphate (KH_2PO_4, ⩾99%), Dipotassium hydrogenphosphate ($K_2H_PO_4$, 99.0%)

Material characterization

The crystal structures of the prepared materials were identified by X-ray diffraction (XRD). The morphological information of the samples was revealed by scanning electron microscopy (SEM) and transmission electron microscopy (TEM). The chemical compositions were analyzed by energy dispersive X-ray (EDS) and X-ray photoelectron spectroscopy (XPS). The absorbance data of the spectrophotometer are obtained on the ultraviolet-visible (UV) spectrophotometer.

Electrochemical test

Electrochemical measurements were made in a Type H cell separated by a treated bipolar membrane using a CHI 760E electrochemical workstation. The electrolyte solution (20mL) was 0.1M KOH with or without 0.1M NO_3^- (KNO_3). Carbon rod and Hg/HgO electrodes were used as the opposite electrode and reference electrode, respectively, and carbon cloth of 1x1cm^2 load material was cut as the working electrode. According to Nernst equation, all potentials are converted to reversible hydrogen electrode (RHE) potentials ($E_{RHE}=E_{SCE}+0.059\times pH+0.098V$). Linear sweep voltammetry (LSV) scans were performed at a scanning rate of 10mV·s^{-1} from -0.5 to -1.8V in the electrolyte containing and without 0.1M NO_3^- in 0.1M KOH, respectively.

Product quantification:

The UV-VIS spectrophotometer is used to detect the ion concentration of the electrolyte after dilution to the appropriate concentration test to match the range of the calibration curve. Specific detection methods are as follows:

Detection of NH_4^+-N:

The concentration of NH_3 was determined by indigo blue spectrophotometry. After the reaction, the diluted electrolyte was first added to it by drops of 2mL 1M NaOH solution containing 5.0wt % sodium citrate and 5.0wt % salicylic acid, and then added to it by drops of 0.2mL solution containing 1wt% sodium nitroprusside. Finally, 0.05M $NaClO\cdot 5H_2O$

solution 1mL was added to it by drops, and the colorimetric tube was shaken to make the solution mixed evenly. The solution was kept in a dark and draftless place for 1~2 h to make the color develop completely. The absorbance was measured by UV-vis spectrophotometry at 655nm, and the standard NH_4Cl solution was used to draw the NH_3 standard absorption curve according to the absorbance corresponding to different concentrations of 0.01~0.1M, thus fitting the curve y = 7.5887x + 0.1411, as shown in the figure below.

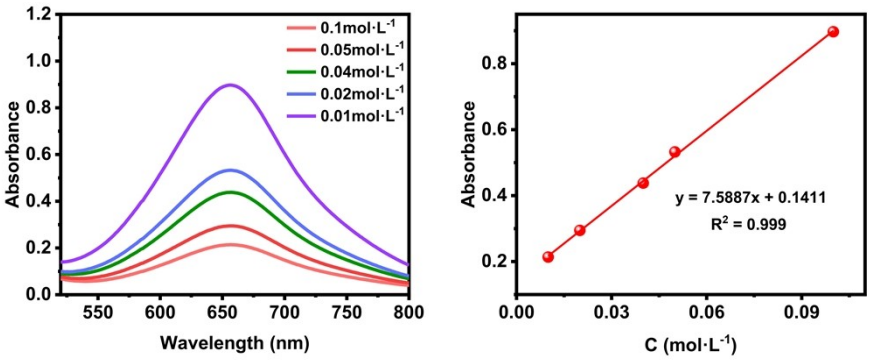

Fig.T1 The full spectrum and standard curve of NH_4^+ using UV-visible spectroscopy.

Detection of NO_2^--N

The configuration of the color developer is as follows: dissolve 4g sulfonamide in a mixture of 50mL deionized water and 10mL phosphoric acid, and then dissolve 0.2g naphthalene ethylenediamine hydrochloride in the above solution. Finally, the solution was transferred to a 100mL volumetric bottle to obtain nitrite color developing agent. The reaction electrolyte was removed from the electrolytic cell and diluted to the detection range. 5mL of the diluted electrolyte solution was put into the colorimetric tube, and 0.2mL of the above chromogenic agent was added to it. The colorimetric tube was shaken to make the solution evenly mixed, and the solution was kept in a dark and draft-free place for 1~2 hours until the color development was complete. The absorbance was measured by UV-vis spectrophotometry at 540nm. Standard $NaNO_2$ solution was used to draw the NO_2^--N standard absorption curve according to different concentrations of 0.01~0.025M corresponding to absorbance, so as to fit the curve y =41.023x+0.0229, as shown in the figure

below.

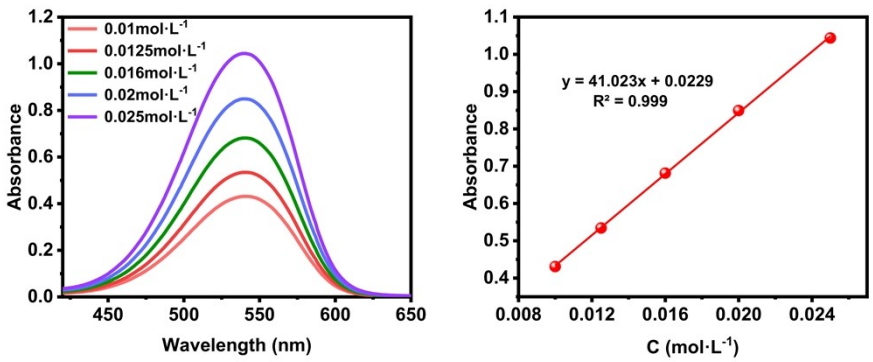

Fig.T2 The full spectrum and standard curve of nitrite (NO_2^-) using UV-visible spectroscopy.

Calculation of yield, selectivity and Faraday efficiency:

FE for NO_3^- reduction is defined as the amount of charge used to synthesize NH_3 divided by the total charge passing through the electrode during electrolysis.

The total amount of NH_3 produced was measured using colorimetry. FE towards NH_3 via NO_3RR is calculated by the following equation:

$$FE = \frac{8 * F * C * V}{Q}$$

NH_3 yield was calculated using the following formula:

$$NH_3\ yield = \frac{17 * C * V}{t * A}$$

Where, F is Faraday constant (96485 C·mol^{-1}), C is the concentration of NH_3 measured in the electrolyte after the antisense, V is the volume of the electrolyte measured in the cathode chamber (0.02L), 17 is the molar mass of NH_3, Q is the total charge passing through the electrode per unit time, t is the electrolytic time, A is the loading area of the catalyst (0.1×0.1 cm^2).

Calculation of Faradaic Efficiency for H_2 and N_2:

To determine the Faradaic efficiency of H_2 and N_2 during the NO_3RR reaction, we employed a gas collection method to gather H_2 and N_2. The Faradaic efficiency for NO_3RR was

calculated using the following formula:

$$FE = \frac{N_{gas\ volume}}{Q_{total}/(Z \times F)} \times 100\%$$

Where Q_{total} is the total charge passed through the electrode during the reaction, Z is the number of electrons required for the generation of gas molecules (Z_{H2} is 2, Z_{N2} is 10), and F is the Faraday constant (96485 C mol^{-1}).

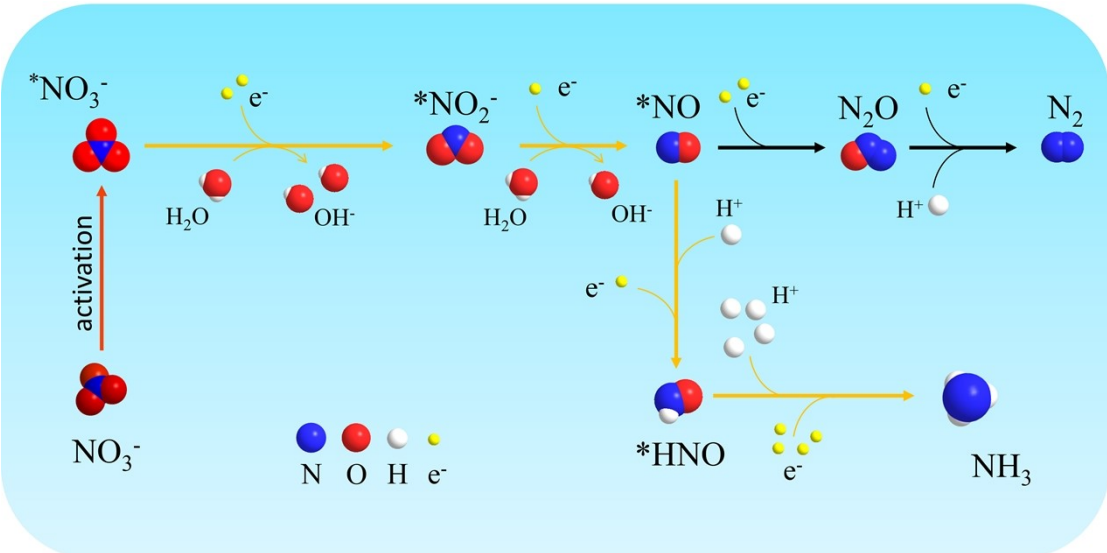

Fig. S1 NO_3^- reduced ammonia production pathway

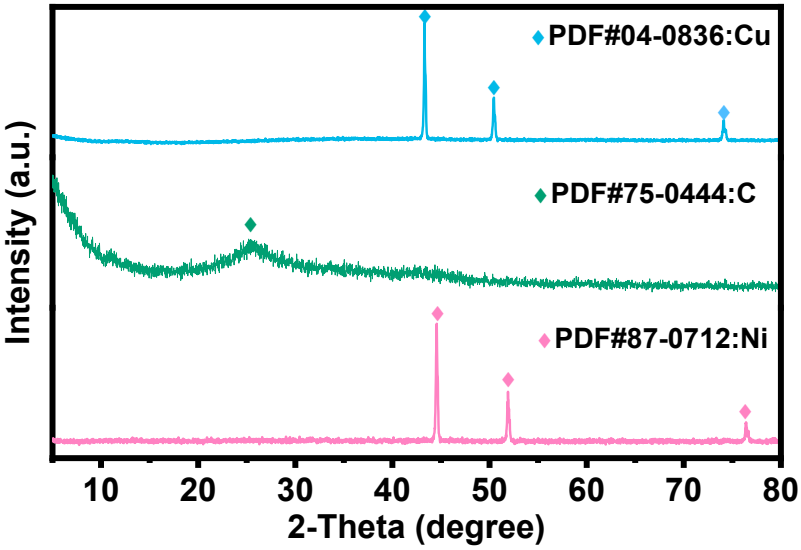

Fig.S2 XRD diffraction patterns of Co@CF, Co@CC and Co@NF.

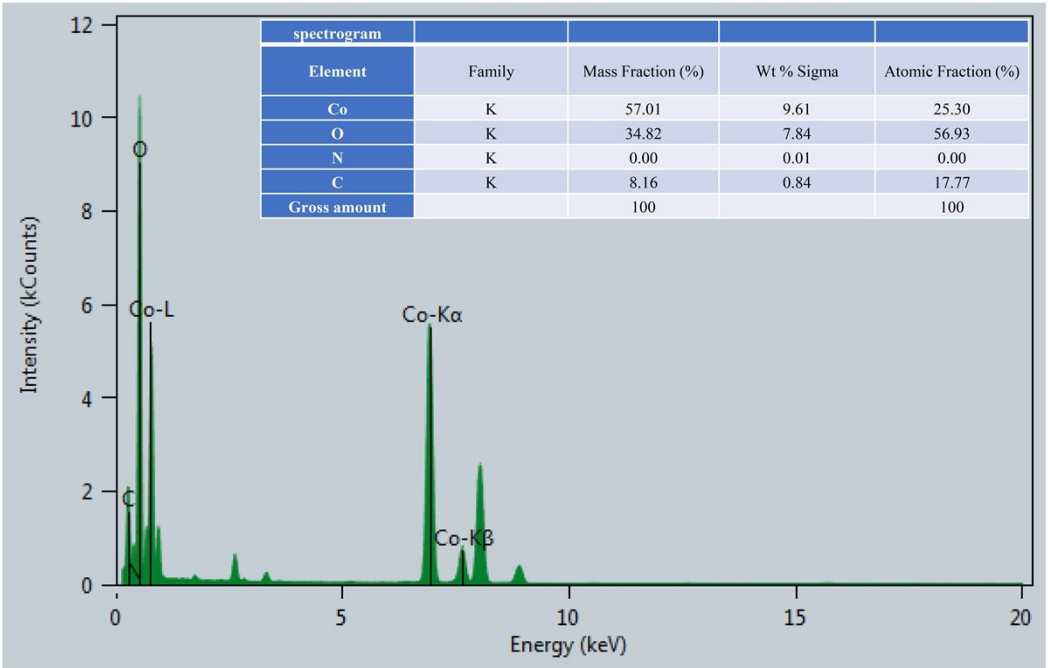

spectrogram				
Element	Family	Mass Fraction (%)	Wt % Sigma	Atomic Fraction (%)
Co	K	57.01	9.61	25.30
O	K	34.82	7.84	56.93
N	K	0.00	0.01	0.00
C	K	8.16	0.84	17.77
Gross amount		100		100

Fig.S3 The EDS spectra for Co@CF under transmission electron microscopy.

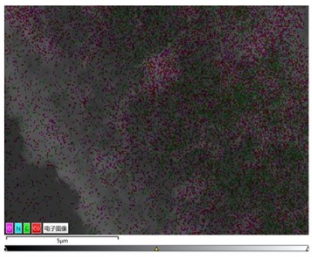

spectrogram				
Element	Family	Mass Fraction (%)	Wt % Sigma	Atomic Fraction (%)
Co	L	37.78	0.75	12.15
C	K	35.37	0.61	55.81
N	K	1.33	0.64	1.79
O	K	25.53	0.48	30.24
Gross amount		100.00		100.00

Fig.S4 The EDS spectra for Co@CC under SEM.

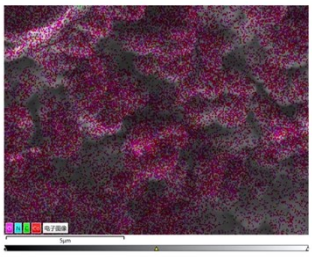

spectrogram				
Element	Family	Mass Fraction (%)	Wt % Sigma	Atomic Fraction (%)
Co	L	64.76	0.59	32.07
C	K	5.05	0.36	12.26
N	K	2.28	0.33	4.75
O	K	27.91	0.45	50.92
Gross amount		100.00		100.00

Fig.S5 The EDS spectra for Co@NF under SEM.

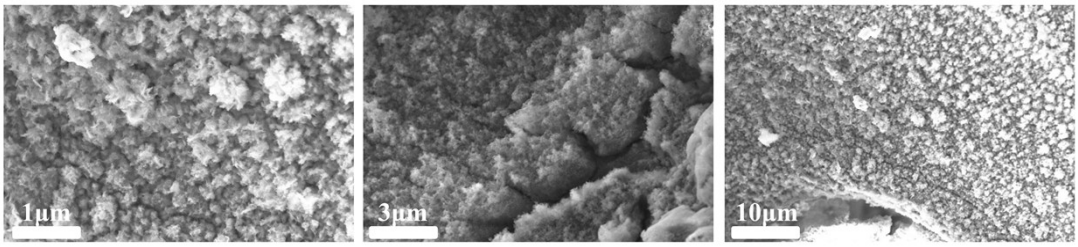

Fig.S6 SEM image of Co@CF.

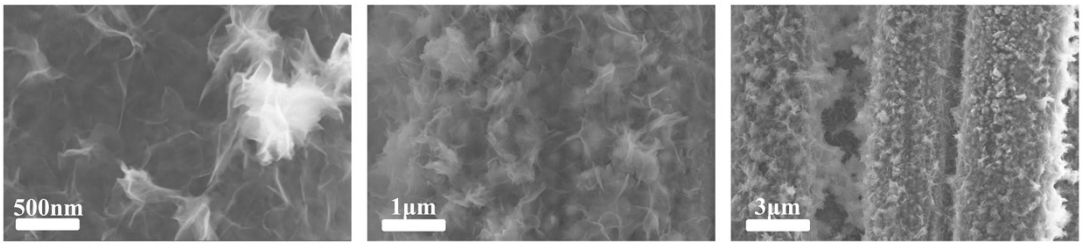

Fig.S7 SEM image of Co@CC.

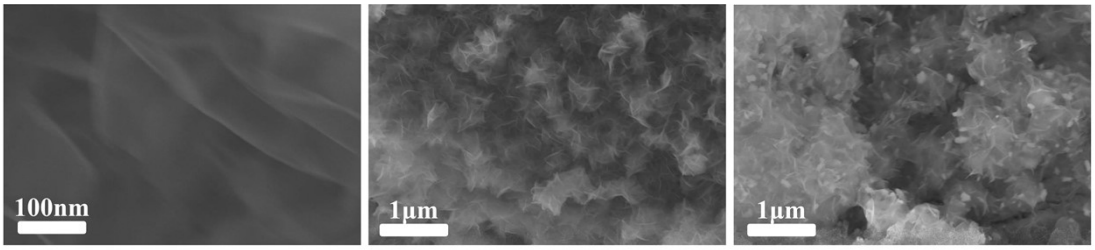

Fig.S8 SEM image of Co@NF.

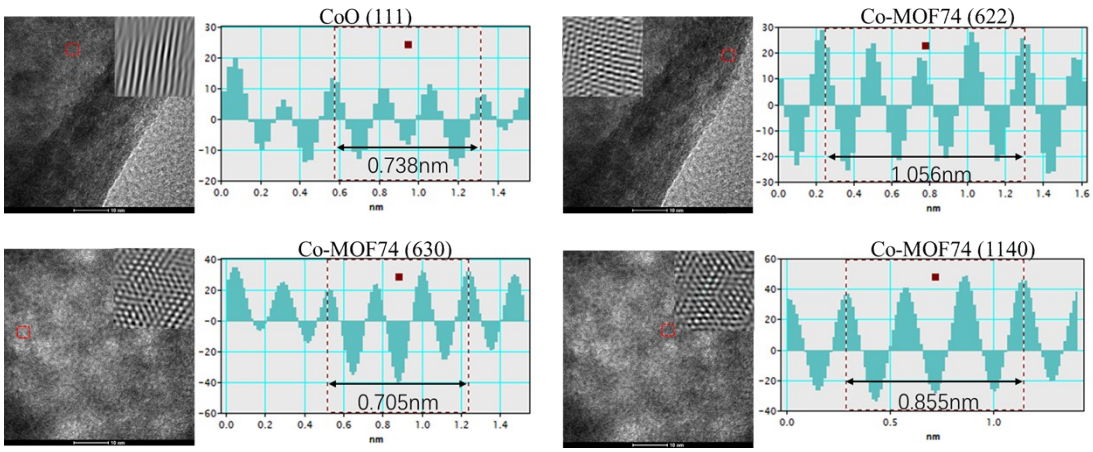

Fig.S9 The lattice spacing of Co@CF

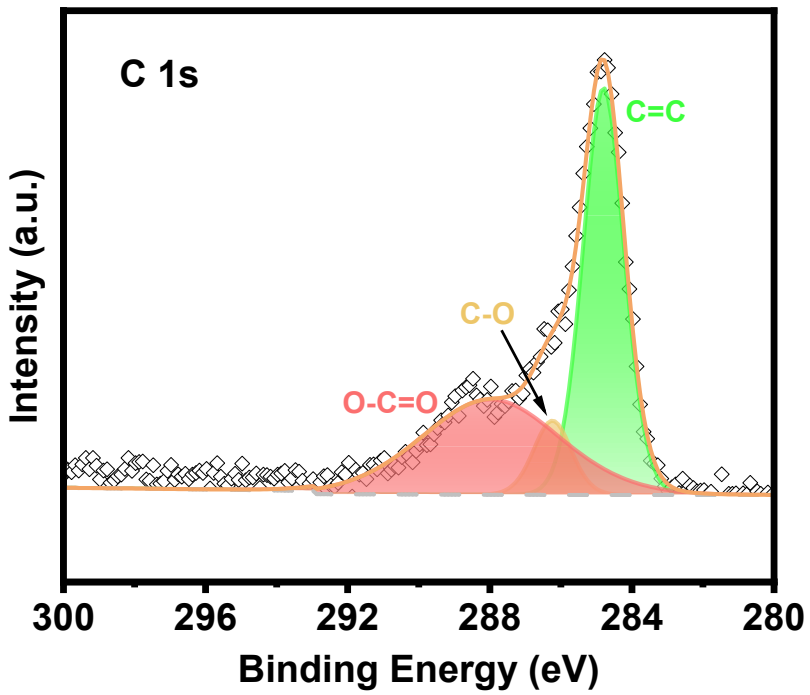

Fig.S10 XPS of Co@CF, C spectrum

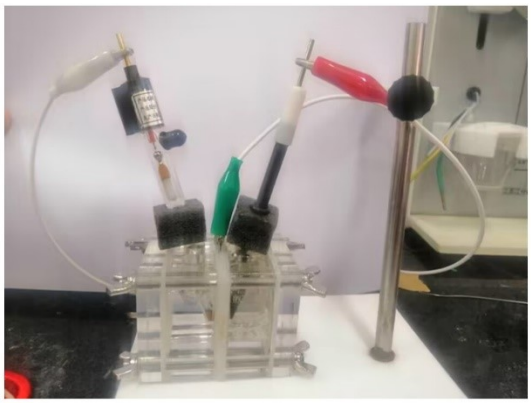

Fig.S11 Self-assembled H-type electrolysis cell.

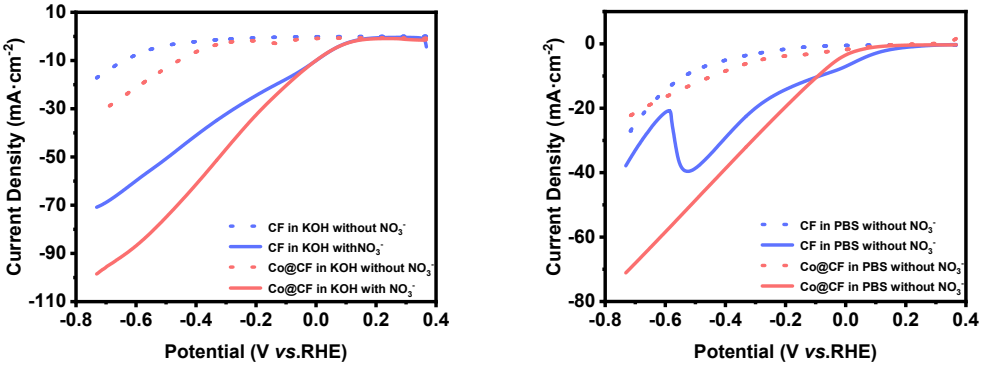

Fig.S12 The LSV of Co@CF in 0.1 M KOH and 0.1 M PBS solutions.

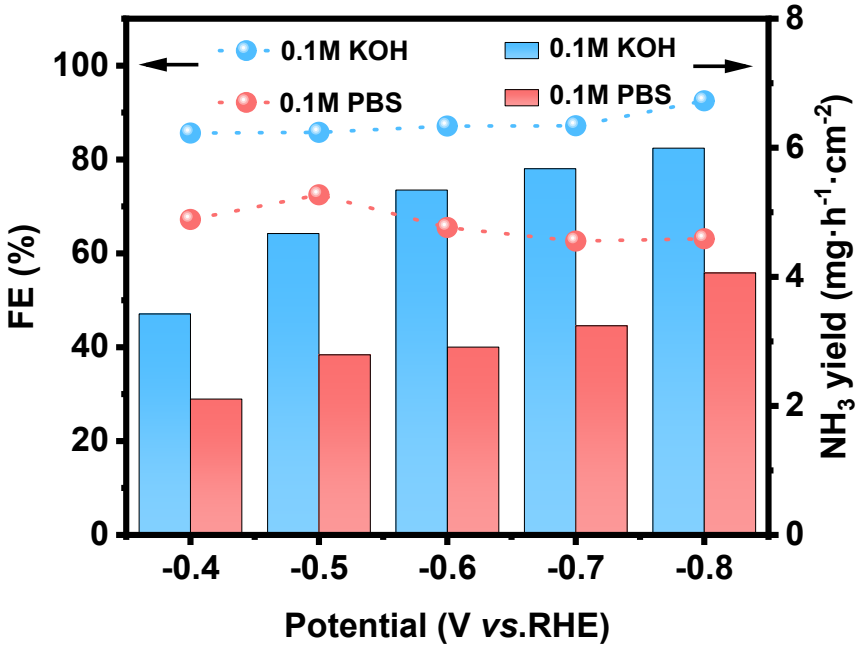

Fig.S13 FEs and NH_3 yield of Co@CF in 0.1M KOH and 0.1M PBS.

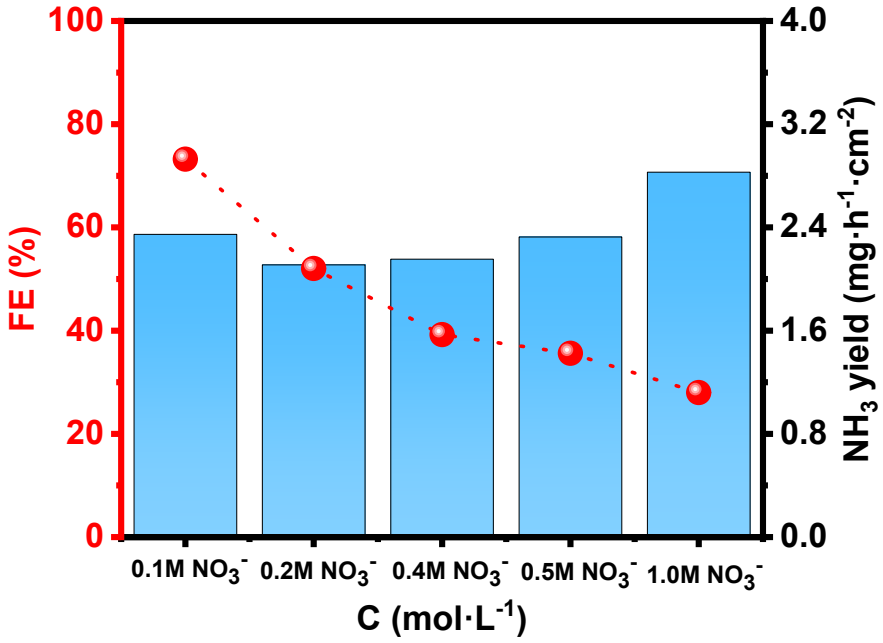

Fig.S14 FEs and NH_3 yield of Co@CF in different nitrate concentrations.

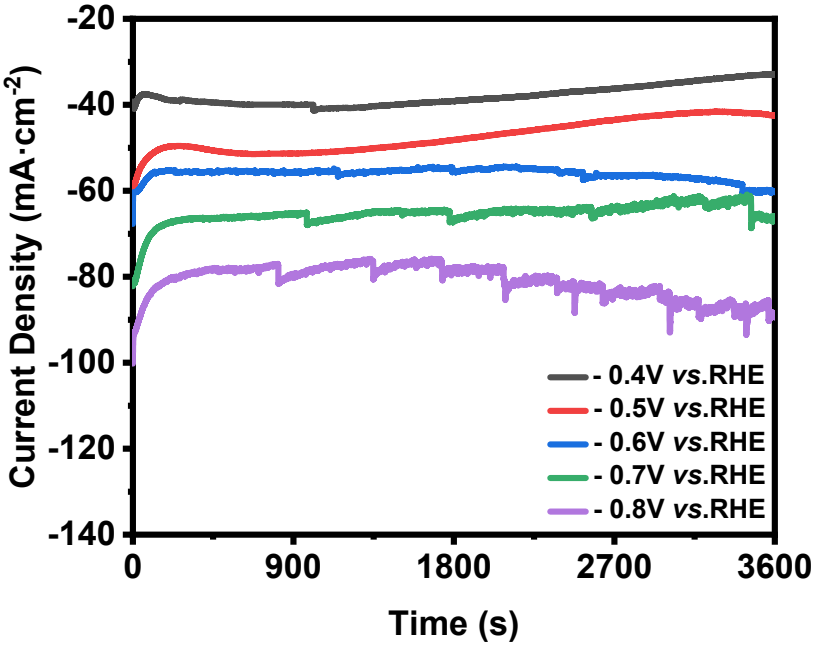

Fig.S15 The Chronoamperometric curves of Co@CF at various potentials (-0.4 V *vs* RHE to -0.8 V *vs*. RHE).

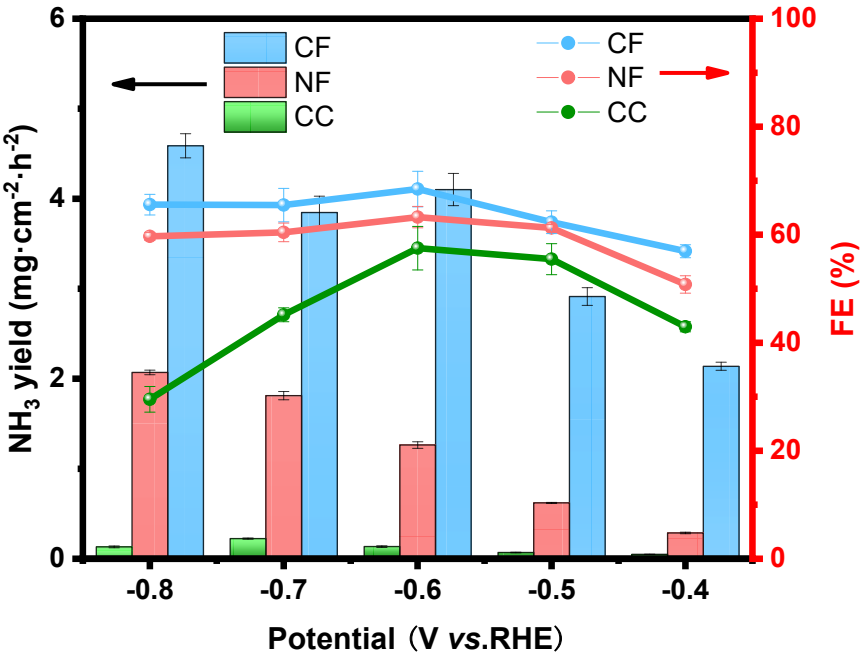

Fig. S16 Ammonia production rates for CC, NF and CF and FE.

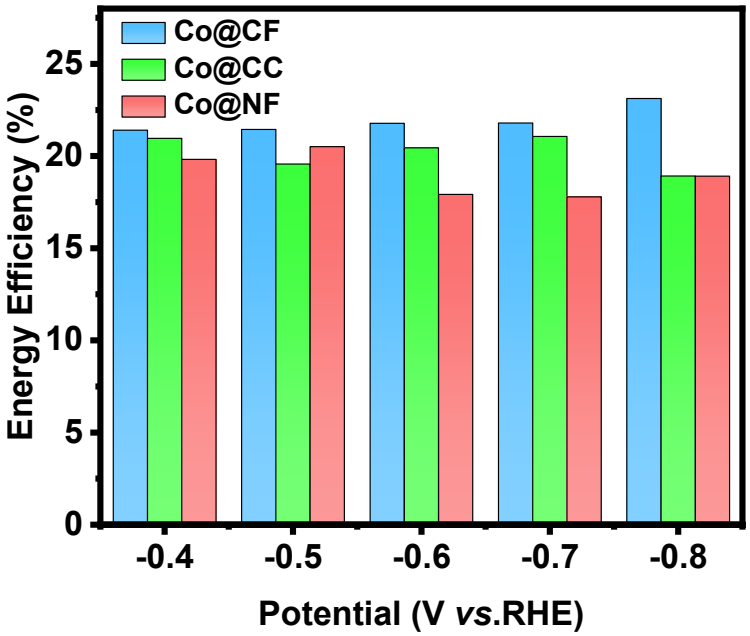

Fig.S17 The energy efficiency for nitrate reduction to ammonia based on Co@CF，Co@CC and Co@NF.

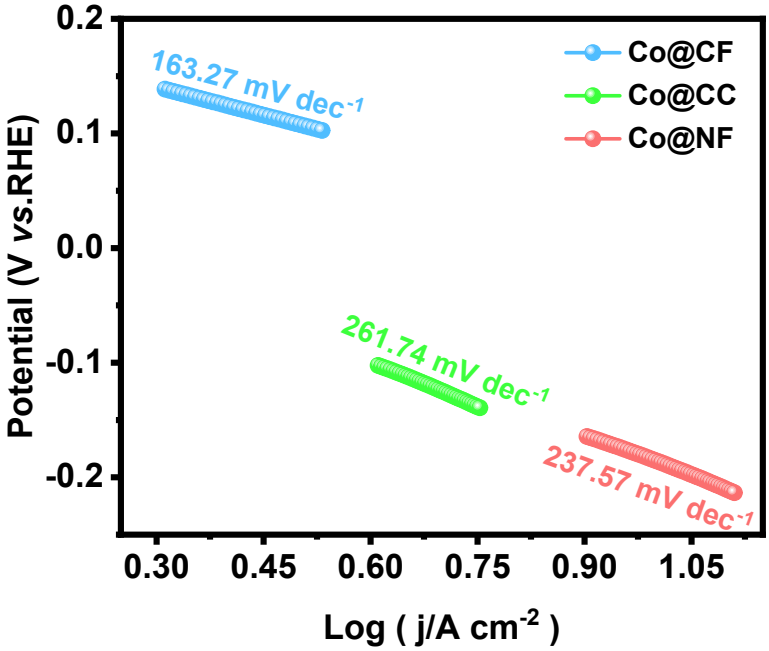

Fig.S18 Tafel plots of Co@CF, Co@CC and Co@NF.

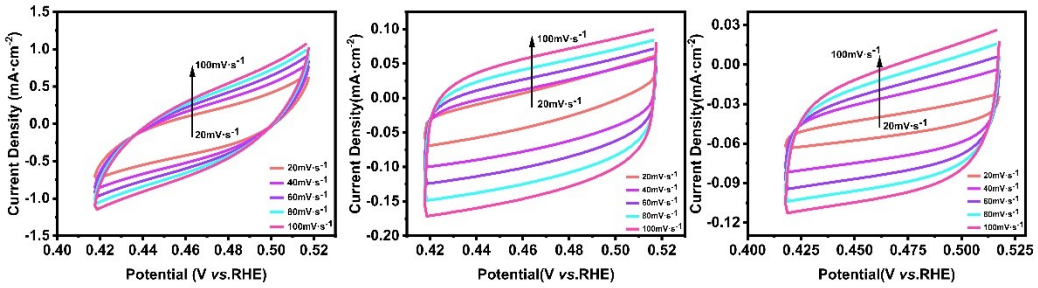

Fig.S19 CV curves of Co@CF, Co@CC and Co@NF with different scan rates from 20 to 100 mV/s.

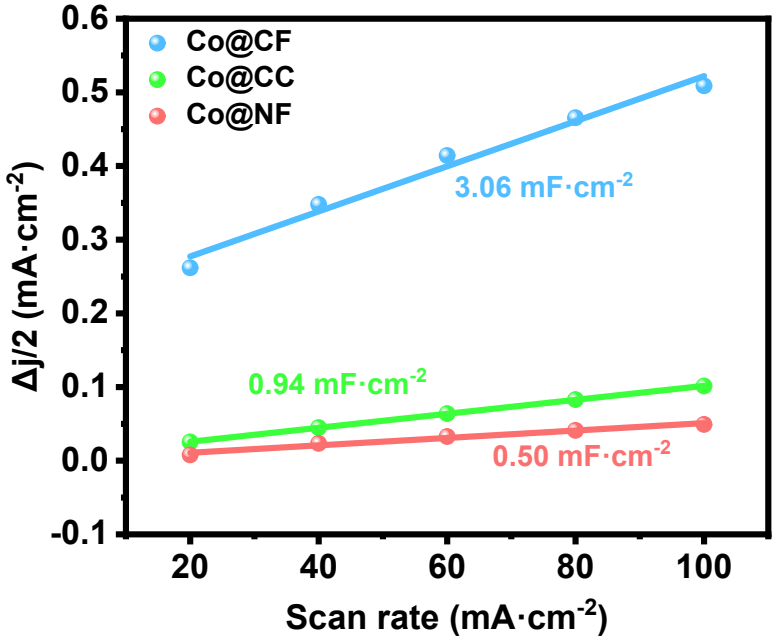

Fig.S20 Capacitive current as a function of the scanrates.

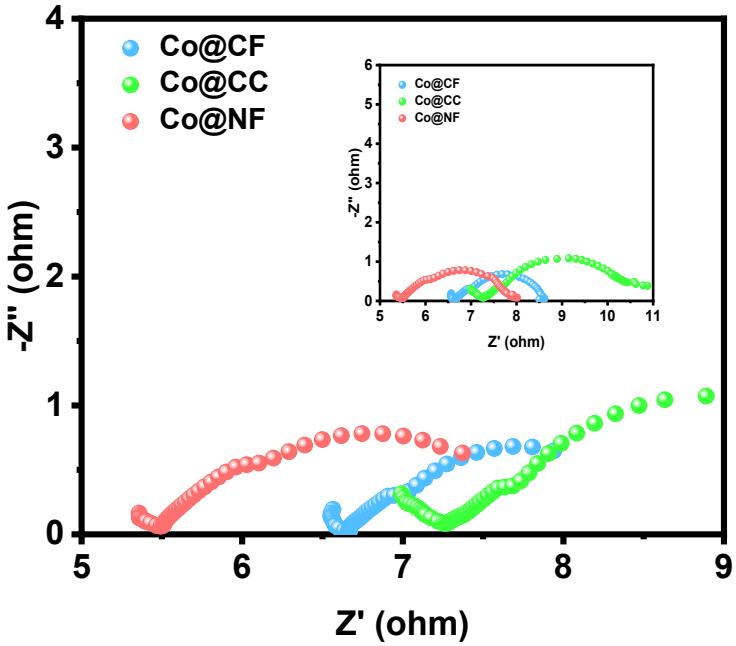

Fig.S21 Nyquist plots of Co@CF, Co@CC and Co@NF

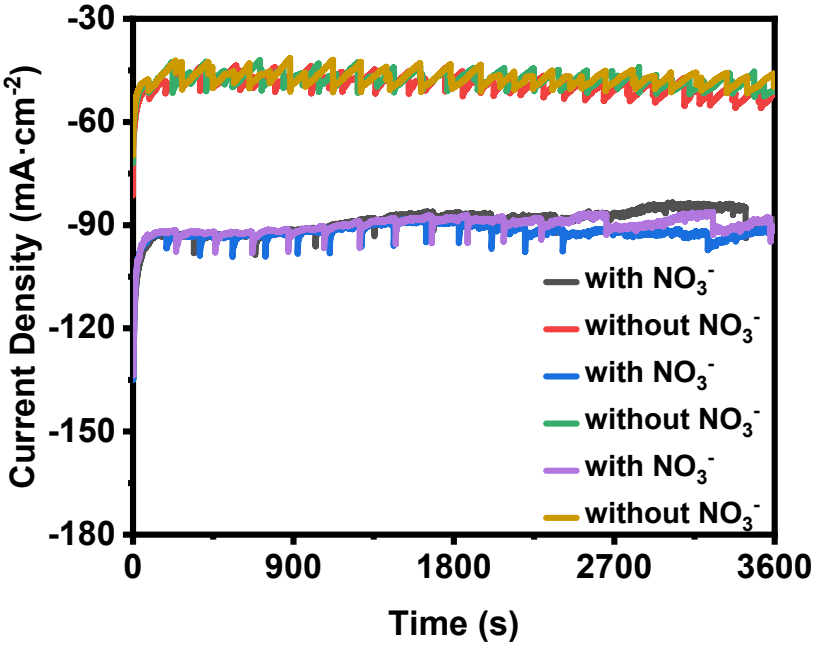

Fig.S22 Chronoamperometric curves of Co@CF in nitrate-N solution (with NO_3^-) and blank solution (without NO_3^-) for six times.

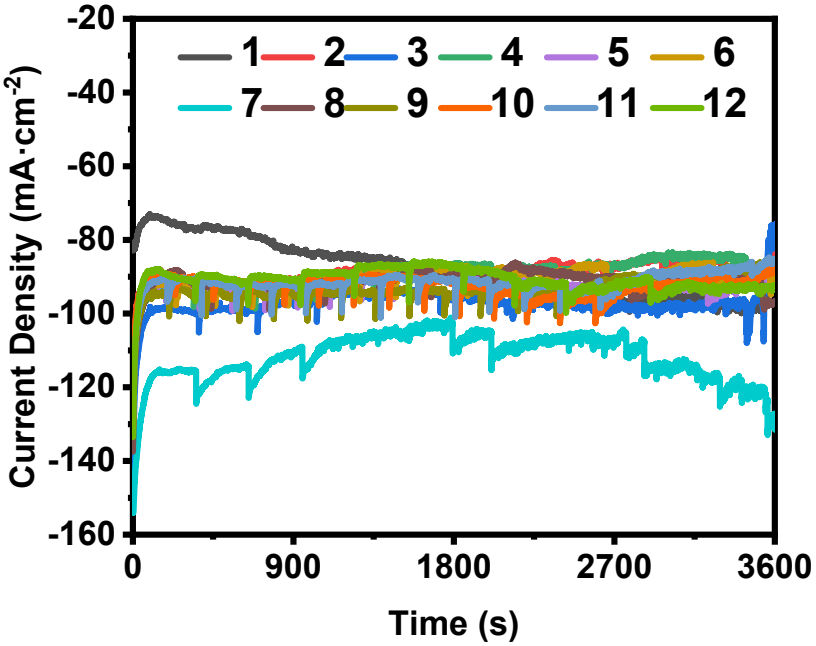

Fig.S23 Cyclic stability tests of Co@CF: Chronoamperometry curves for twelve times at -0.8V *vs*.RHE.

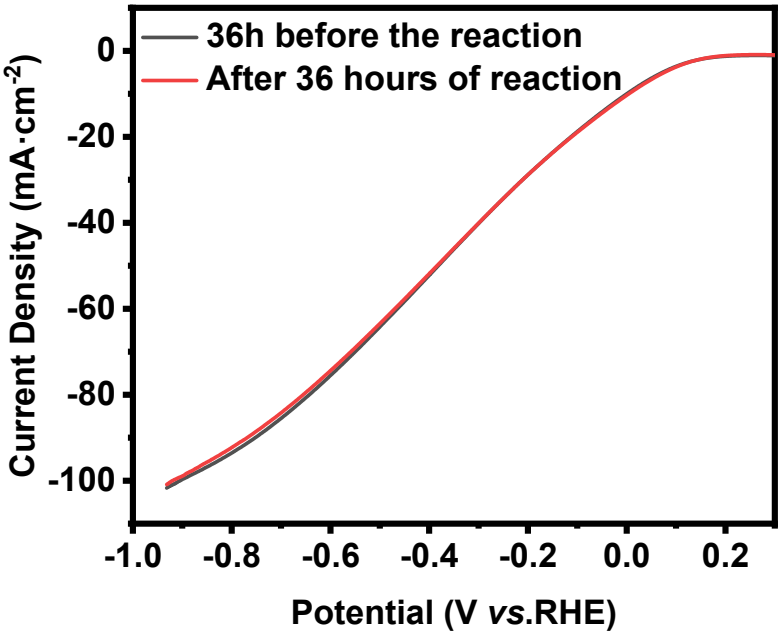

Fig.S24 LSV of Co@CF before and after 36h reduction reaction

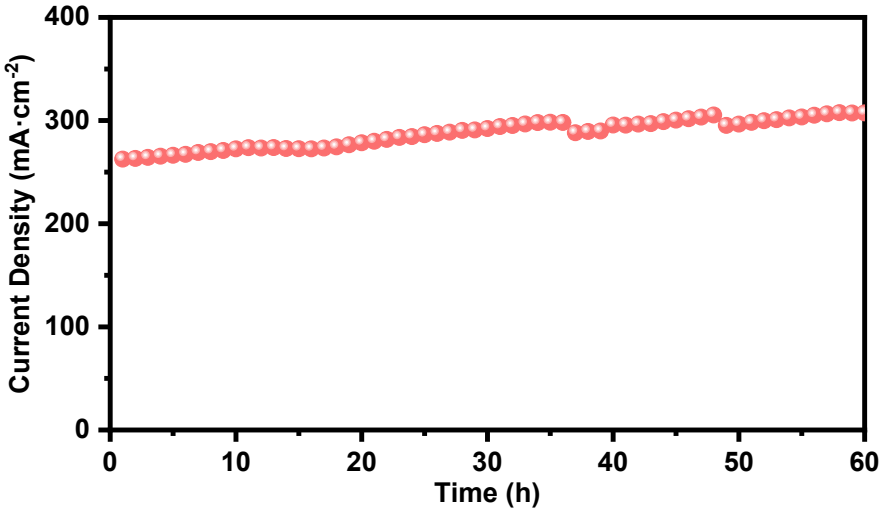

Fig.S25 Evolution of current density over time for continuous electrolysis of 60 h.

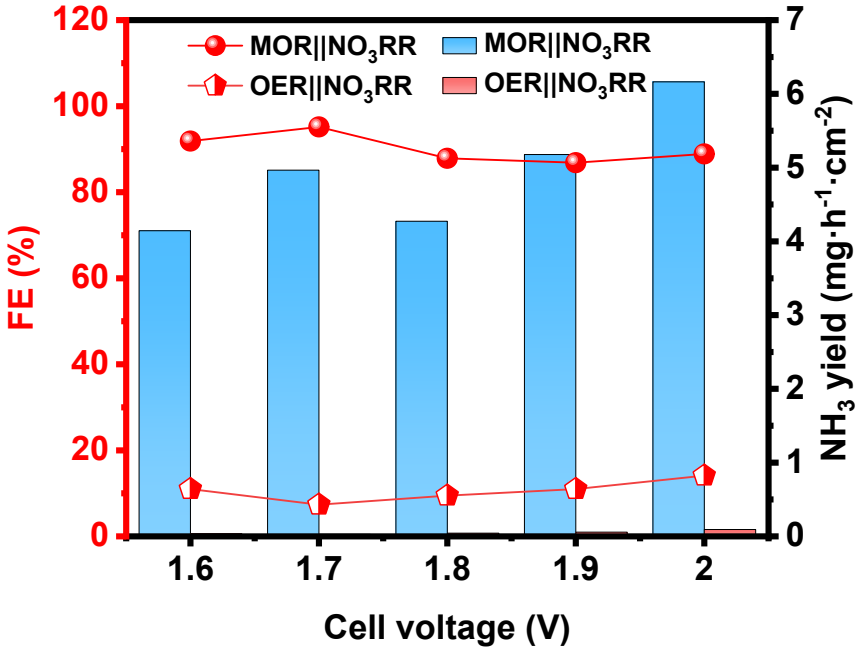

Fig.S26 FEs and NH_3 yield of MOR||NO_3RR and OER||NO_3RR.

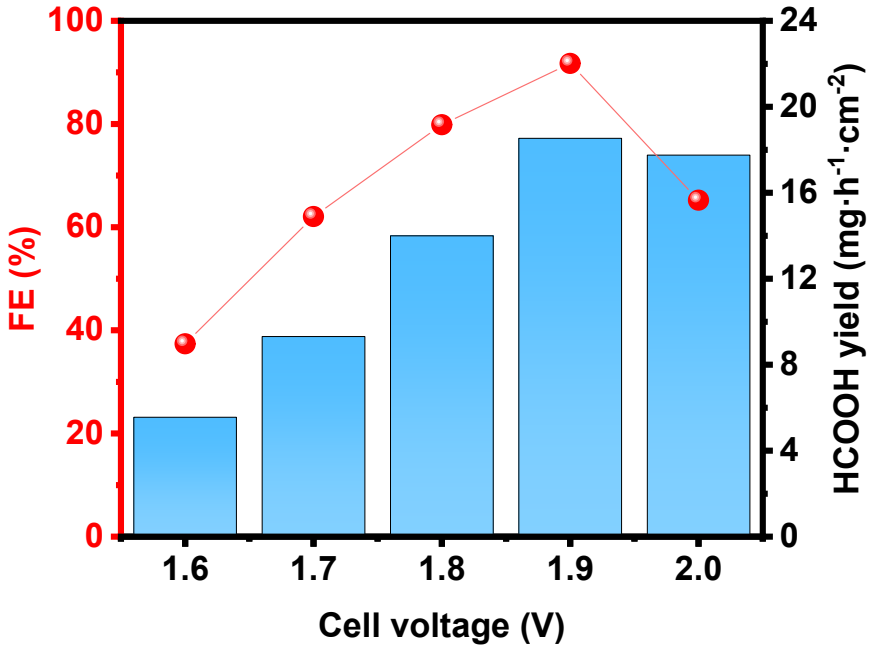

Fig.S27 Yield and FEs of HCOOH at anode.

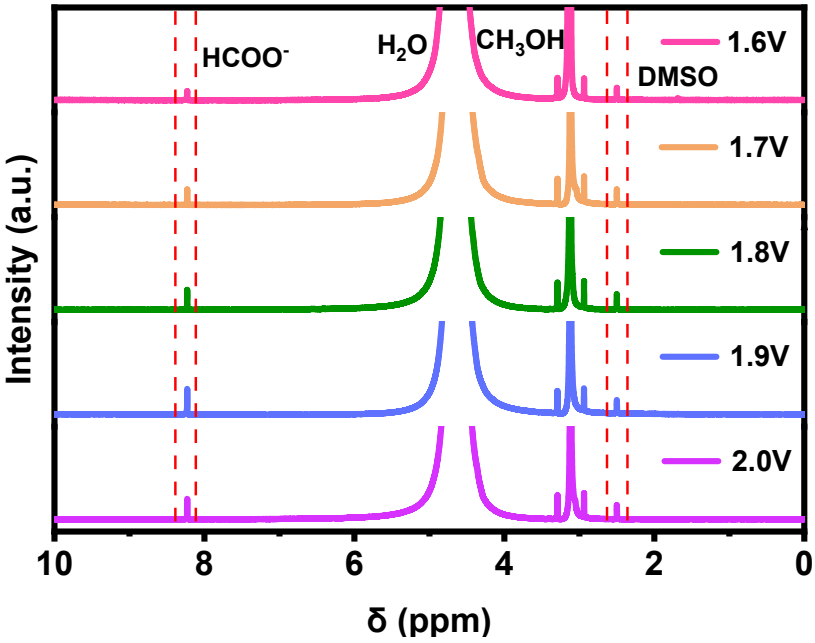

Fig.S28 The 1H-NMR spectrum of the anode electrolyte obtained after MOR by Co@CF at different potentials

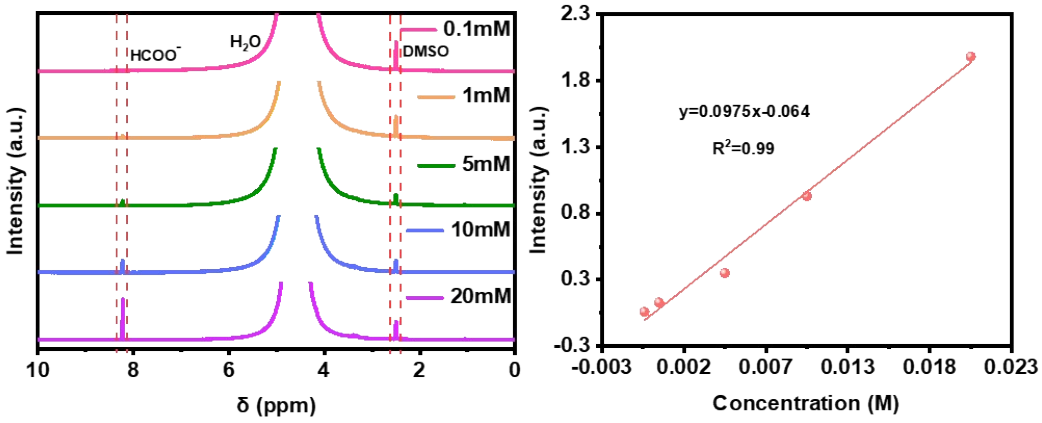

Fig.S29 ^{1}H-NMR spectra of formic acid standard curve.

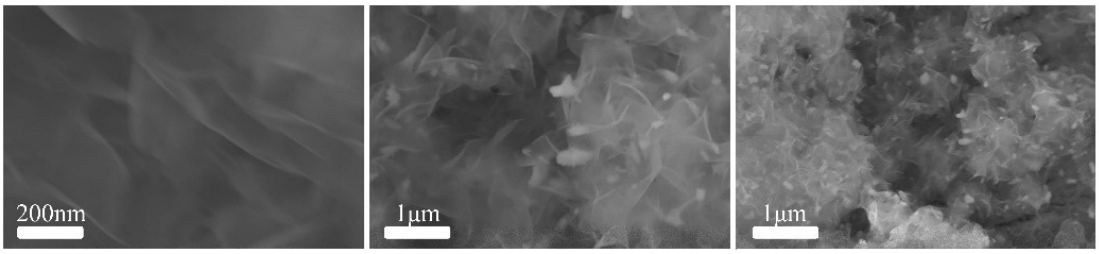

Fig.S30 SEM of Co@CF after 50h of NO_3RR reaction

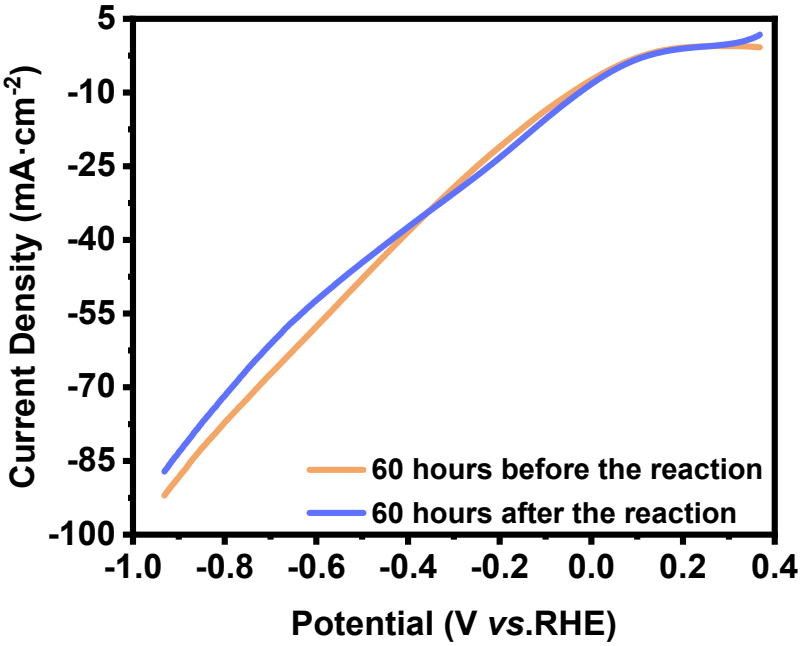

Fig.S31 LSV of Co@CF before and after 60h of NO_3RR reaction

Table S1. Results of ICP analyses of cobalt on different substrates

Sample number	Sample quality m_0 (g)	Test elements	Test the solution for the elemental concentration Co (ug/L)	Sample element content Cx (mg/kg)	Sample element content W%
1-CC	0.0582	Co	20.1286	3.46	0.0003%
2-NF	0.0714	Co	39.1449	5.48	0.0005%
3-CF	0.0536	Co	4.2666	0.80	0.0001%

Table S2. Summary of published performance plots of materials for ammonia production by electrocatalytic nitrate reduction

Cathode Material	FE to NH_3	Current Density $mA \cdot cm^{-2}$	NH_3 production Repoted	Condition	Potential V *vs*.RHE	Ref.
Co@CF	92.5%	-104.5	5.99 $mg \cdot h^{-1} \cdot cm^{-2}$	0.1M KNO_3 0.1M KOH	-0.8	This work
Co@CC	83.8%	-65.2	3.40 $mg \cdot h^{-1} \cdot cm^{-2}$	0.1M KNO_3 0.1M KOH	-0.7	This work
Co@NF	82.1%	51.1	3.35 $mg \cdot h^{-1} \cdot cm^{-2}$	0.1M KNO_3 0.1M KOH	-0.5	This work
Cu foil	30%	~-0.36	3.9 $\mu g \cdot mg_{cat}^{-1} \cdot h^{-1}$ （3.9 $\mu g \cdot h^{-1} \cdot cm^{-2}$）	10mM KNO_3 0.1M KOH	-0.15	[1]
Cu SAC	84.7%	~−75	0.26 $mmol \cdot cm^{-2} \cdot h^{-1}$ (12.5 $mol \cdot g_{Cu}^{-1} \cdot h^{-1}$)	0.1M KNO_3 0.1M KOH	-1.00	[2]
Cu-incorporated PTCDA	77%	-	0.0256 $mmol \cdot h^{-1} \cdot cm^{-2}$	0.1mM PBS, 36mM NO_3^-	-0.4	[3]
FOSP-Cu	93.9%	-	101.4 $\mu mol \cdot h^{-1} \cdot cm^{-2}$	0.1M KNO_3 0.5M Na_2SO_4	-0.266	[4]
CuNS/CC	93.5%	21.6	0.03 $mmol \cdot h^{-1} \cdot cm^{-2}$	200ppm KNO_3 0.5M K_2SO_4	-0.65	[5]
Mo_2C/RGO	85.2%	59.8	4.8 $mg \cdot h^{-1} \cdot cm^{-2}$	0.1M KNO_3 0.5M Na_2SO_4	-0.6	[6]
S-modified FeSAC	78.4%	1.2	95.1 $\mu g \cdot h^{-1} \cdot cm^{-2}$	0.0071$mg \cdot L^{-1}$ NO_3^-	-0.67	[7]
CuSANPC	94.1%	-	2602 $\mu g \cdot h^{-1} \cdot cm^{-2}$	0.01M PBS 500$mg \cdot L^{-1}$ NO_3^-	-1.1	[8]
Fe SAC	86%	60.7	4812 $\mu g \cdot h^{-1} \cdot cm^{-2}$	0.5$mg \cdot L^{-1}$ NO_3^-	-	[9]
$Cu_{50}Ni_{50}$	82.0%	-	80.7$\mu mol \cdot h^{-1} \cdot cm^{-2}$	1M KOH 100mM KNO_3	–0.1	[10]

[1] X. Fu, X. Zhao, X. Hu, K. He, Y. Yu, T. Li, Q. Tu, X. Qian, Q. Yue, M.R. Wasielewski, Y. Kang, Alternative route for electrochemical ammonia synthesis by reduction of nitrate on copper nanosheets, Applied Materials Today 19 (2020).
[2] J. Yang, H. Qi, A. Li, X. Liu, X. Yang, S. Zhang, Q. Zhao, Q. Jiang, Y. Su, L. Zhang, J.F. Li, Z.Q. Tian, W. Liu, A. Wang, T. Zhang, Potential-Driven Restructuring of Cu Single Atoms to Nanoparticles for Boosting the Electrochemical Reduction of Nitrate to Ammonia, J Am Chem Soc 144 (2022) 12062-12071.
[3] G.-F. Chen, Y. Yuan, H. Jiang, S.-Y. Ren, L.-X. Ding, L. Ma, T. Wu, J. Lu, H. Wang, Electrochemical reduction of nitrate to ammonia via direct eight-electron transfer using a copper–molecular solid catalyst, Nature Energy 5 (2020) 605-613.
[4] Y. Zhao, Y. Liu, Z. Zhang, Z. Mo, C. Wang, S. Gao, Flower-like open-structured polycrystalline copper with synergistic multi-crystal plane for efficient electrocatalytic reduction of nitrate to ammonia, Nano Energy 97 (2022).
[5] J. Cai, Y. Wei, A. Cao, J. Huang, Z. Jiang, S. Lu, S.-Q. Zang, Electrocatalytic nitrate-to-ammonia conversion with ~100% Faradaic efficiency via single-atom alloying, Applied Catalysis B: Environmental 316 (2022).
[6] X. Li, S. Wang, G. Wang, P. Shen, D. Ma, K. Chu, Mo(2)C for electrocatalytic nitrate reduction to ammonia, Dalton Trans 51 (2022) 17547-17552.
[7] J. Li, M. Li, N. An, S. Zhang, Q. Song, Y. Yang, X. Liu, Atomically dispersed Fe atoms anchored on S and N-codoped carbon for efficient electrochemical denitrification, Proc Natl Acad Sci U S A 118 (2021).
[8] X. Zhao, Q. Geng, F. Dong, K. Zhao, S. Chen, H. Yu, X. Quan, Boosting the selectivity and efficiency of nitrate reduction to ammonia with a single-atom Cu electrocatalyst, Chemical Engineering Journal 466 (2023).
[9] Z.Y. Wu, M. Karamad, X. Yong, Q. Huang, D.A. Cullen, P. Zhu, C. Xia, Q. Xiao, M. Shakouri, F.Y. Chen, J.Y.T. Kim, Y. Xia, K. Heck, Y. Hu, M.S. Wong, Q. Li, I. Gates, S. Siahrostami, H. Wang, Electrochemical ammonia synthesis via nitrate reduction on Fe single atom catalyst, Nat Commun 12 (2021) 2870.
[10] Y. Wang, A. Xu, Z. Wang, L. Huang, J. Li, F. Li, J. Wicks, M. Luo, D.H. Nam, C.S. Tan, Y. Ding, J. Wu, Y. Lum, C.T. Dinh, D. Sinton, G. Zheng, E.H. Sargent, Enhanced Nitrate-to-Ammonia Activity on Copper-Nickel Alloys via Tuning of Intermediate Adsorption, J Am Chem Soc 142 (2020) 5702-5708.